SYNTHESIS OF NANOSIZED BISMUTH FERRITE (BiFeO$_3$) BY A COMBUSTION METHOD STARTING FROM Fe(NO$_3$)$_3$·9H$_2$O–Bi(NO$_3$)$_3$·9H$_2$O–GLYCINE OR UREA SYSTEMS

Carmen Paraschiv[1]*, B. Jurca*[2]*, Adelina Ianculescu*[3] *and Oana Carp*[1]*

[1]Institute of Physical Chemistry, Splaiul Independentei No. 202, 060021 Bucharest, Romania
[2]Department of Physical Chemistry, Faculty of Chemistry, University of Bucharest, Bd. Elisabeta No. 12, 030017 Bucharest, Roumania
[3]University Politehnica of Bucharest, Gh.Polizu Street No. 1–7, 011061 Bucharest, Romania

Two bismuth ferrite potential precursors systems, namely Fe(NO$_3$)$_3$·9H$_2$O – Bi(NO$_3$)$_3$·9H$_2$O – glycine/urea with different metal nitrate/organic compound molar ratios have been investigated in order to evaluate their suitability as BiFeO$_3$ precursors. The presence into the precursor of both reducing (glycine and urea) and oxidizing (NO$_3^-$) components, modifies dramatically their thermal behaviour comparative with the raw materials, both from the decomposition stoichiometries and temperature occurrence intervals points of view. Also, the thermal behaviour is dependent on the fuel nature but practically independent with the fuel content. The fuel nature influences also some characteristics of the resulted oxides (phase composition, morphologies). In the case of the oxides prepared using urea as fuel, a faster evolution toward a single phase composition with the temperature rise is evidenced, the formation of the BiFeO$_3$ perovskite phase being completed in the temperature range of 500–550°C.

Introduction

Bismuth ferrite, (BiFeO$_3$, BFO) is one of the very few multiferroics materials with a simultaneous coexistence of ferroelectric and antiferromagnetic order parameters in perovskite structure. Although BFO was discovered in 1960, recently there is a renewed interest because of its possible novel applications in the field of radio, television, microwave and satellite communications, audio-video and digital recording and, as permanent magnets.

So far, bismuth ferrite powders have been prepared by the solid-state methods (classic [1, 2] and mechanochemical ones [3]) and solution chemistry methods (such as precipitation/coprecipitation [4], sol–gel [5, 6] hydrothermal [7] and sonochemical [8] ones). Most of the mentioned procedures need high temperature treatments (>800°C). Due to the requirement of nanosized oxides and in order to avoid bismuth volatilization the developing of low temperature synthesis methods is essential.

In the present paper we report the synthesis of bismuth ferrite by a simple combustion technique, using as starting system Fe(NO$_3$)$_3$·9H$_2$O– Bi(NO$_3$)$_3$·9H$_2$O as oxidizer and glycine or urea as fuels. Because the synthesis of mixed oxide is determined by a combustion reaction, a special attention is paid to the thermal reactivity of the precursor and solid-state mechanism.

Experimental

The synthesis of the BFO precursors was performed using a solid-state method. The starting materials of analytical grade Fe(NO$_3$)$_3$·9H$_2$O (Merck), Bi(NO$_3$)$_3$·9H$_2$O (Reactivul, Romanian company), glycine (Fluka) and urea (Merck) were used without any further purification.. The utilized molar ratios were for Fe(NO$_3$)$_3$·9H$_2$O–Bi(NO$_3$)$_3$·9H$_2$O–glycine system 1:1:2.5, 1:1:3.5 and 1:1:4.5 and, for Fe(NO$_3$)$_3$·9H$_2$O–Bi(NO$_3$)$_3$·9H$_2$O–urea system 1:1:4, 1:1:6, 1:1:8. The compositions were selected in order to obtain fuel lean, stoichiometrically and fuel rich compounds, being calculated by using oxidizing valence (metal nitrates) and reducing valence of urea and glycine (fuels). Accordingly to the concept used in propellant chemistry, the elements H, C and any other metallic cation are considered reducing elements with the corresponding valencies equal with 1, 4 and the valency of the metallic cation in the compound respectively. The element oxygen is considered as an oxidizing element with valency –2. The valency of nitrogen is considered 0. The raw materials are mixed (~30 min) in an agate pestle in order to obtain a homogenous slurry. The homogenization is followed by a drying over P$_2$O$_5$. The precursors were heated at different temperatures (500, 550, 600 and 650°C) for 3 h.

---

*   Author for correspondence: carp@acodarom.ro

Thermal measurements were performed on a Q-1500 Paulik–Paulik–Erdey derivatograph, in static air, at a heating rate of 10°C min^{-1} and with sample mass of ~20 mg. In order to investigate the purity of the mixed oxide phase X-ray diffraction measurements were performed at room temperature with a SHIMADZU XRD 6000 diffractometer, using Ni-filtered CuK$_\alpha$ radiation (λ=1.5418 Å), with a scan step of 0.02° and a counting time of 1 s/step, for 2θ ranged between 20–80°. A HITACHI S2600N scanning electron microscope coupled with EDX was used to analyze the morphology and to check the chemical composition of the powders.

Results and discussion

Thermal behaviour of the raw materials

To estimate the influence of fuels on the thermal behaviour of the BFO precursors, the used raw materials were firstly investigated. The TG, DTG and DTA curves of the $Fe(NO_3)_3 \cdot 9H_2O$, $Bi(NO_3)_3 \cdot 5H_2O$, glycine and urea are presented in the Figs 1a–d.

Iron nitrate nonahydrate ($Fe(NO_3)_3 \cdot 9H_2O$) decomposes after melting (56.4°C). Five endothermic decomposition steps were evidenced in the temperature range of 60.6–714.0°C (Fig. 1a). The first decomposition step (60.6–132.2°C, $T_{max\ DTG}$=121.1°C and $T_{max\ DTA}$~122°C, shoulder) is a partial dehydration, namely the evolving five water molecules (calc./found=22.27/22.3%) as a consequence of the differently bounding of these molecules. The second step (132.2–170.8°C, $T_{max\ DTG}$=156.7°C and $T_{max\ DTA}$=156.8°C), represents part of nitrate anions decomposition accompanied by the release of the remainder water molecules. The presence of water in system determines a hydrolysis reaction with formation of iron nitrate hydroxide $Fe(OH)_2(NO_3)$ (calc./found=40.09/40.55%). Such intermediates were identified during the thermal decompositions of several d-metal nitrates [9]. The iron nitrate hydroxide intermediate is further converted (170.8–650.0°C, calc./found=14.56/15.59%) into FeOOH, which finally is transformed into α-Fe_2O_3 (650.0–714.2°C, calc./found=2.22/2.82%, $T_{max\ DTG}$=677.0°C and $T_{max\ DTA}$=679.5°C).

During the bismuth nitrate pentahydrate ($Bi(NO_3)_3 \cdot 5H_2O$) decomposition, six mass loss steps and two phase transitions, all associated with endothermic effects were detected up to 819°C (Fig. 1b). The first decomposition step (70.5–130.6°C, $T_{max\ DTG}$=111.2°C and $T_{max\ DTA}$=79.8°C) represents the simultaneously melting and evolving of two water molecules (calc./found=7.42/7.80%). The next two ones (130.6–156.3°C, $T_{max\ DTG}$=145.6°C and

$T_{max\ DTA}$=147.3 and 156.3–458.3°C, $T_{max\ DTG}$=315.2°C and $T_{max\ DTA}$=330.0°C) correspond to the formation of two bismuth nitrates hydroxides, $Bi(OH)(NO_3)_2$ and $Bi(OH)_2(NO_3)$ respectively (calc./found= 20.41/22.10% and calc./found=9.28/9.80%). On further heating, a three-stepped decomposition of these intermediates occurs (458.3–526.4°C, $T_{max\ DTG}$= 497.1°C and $T_{max\ DTA}$=505.3, 526.4–586.8°C, $T_{max\ DTG}$=568.4°C and $T_{max\ DTA}$=574.1, 586.8–682.1°C, $T_{max\ DTG}$=661.8°C and $T_{max\ DTA}$= 656.7°C). As decomposition product, the monoclinic modification of bismuth oxide (α-Bi_2O_3) is formed, which almost instantaneously ($T_{max\ DTA}$=682.6°C) is converted into the cubic one (δ-Bi_2O_3). The last phase transition ($T_{max\ DTA}$=819.0°C) represents the melting of δ-Bi_2O_3.

Glycine decomposes through three steps (229.0–663.9°C), the first acompanied by a sharp endothermic effect, the other two associated with exothermic ones (Fig. 1c). The first step which occurs in the temperature range 229.0–302.3°C ($T_{max\ DTG}$= 259.6°C and $T_{max\ DTA}$=255.2°C) is attributed to the simultaneous melting and, water and amonia elimination (calc./found=46.66/46.1%), results in concordance with some MS and FTIR investigations [10, 11]. It is known that amino acids do not exhibit clean melting point, and during melting they decompose to lower mass compounds. The next two decomposition steps (302.3–446.6°C, mass loss=18.25%, $T_{max\ DTG}$=351.4°C, $T_{max\ DTA}$=3.70.2 and 446.6–663.9°C, mass loss=35.65%, $T_{max\ DTG}$= 558.2°C and $T_{max\ DTA}$=526.1°C) represent the burn up of the remainder carbonaceous products.

The literature mentions that the thermal decomposition of urea is rather complicated, occurring differently function the measurements conditions [12–14]. Six endothermic decomposition steps were identified in our experiments (Fig. 1d) in the temperature range 141.4–608.0°C. The mass losses stages start after the melting of the organic compound (141.4°C). The two stages of mass loss (47.67/40.22%) evidenced in the temperature range 155.0–419.0°C ($T_{max\ DTG}$=228.9 and 250.8°C/$T_{max\ DTG}$=402.0°C and $T_{max\ DTA}$=232.7 and 250.8°C/$T_{max\ DTA}$=411.4°C) may be attributed in concordance with previous TG-MS data [11] to the partial endothermic decomposition of urea into ammonia (NH_3) and cyanic acid (HNCO) as mentioned by reaction 1:

$$H_2N–CO\text{-}NH_2 \rightarrow [NH_4][NCO] \rightarrow NH_3 + HNCO \quad (1)$$

In the same temperature range condensation products, namely biuret and triuret compounds may be formed by the reaction of cyanic acid with the undecomposed urea (reactions 2 and 3), compounds which decompose at higher temperatures [15]. Thus, the next two decomposition stages (419.0–481.9°C
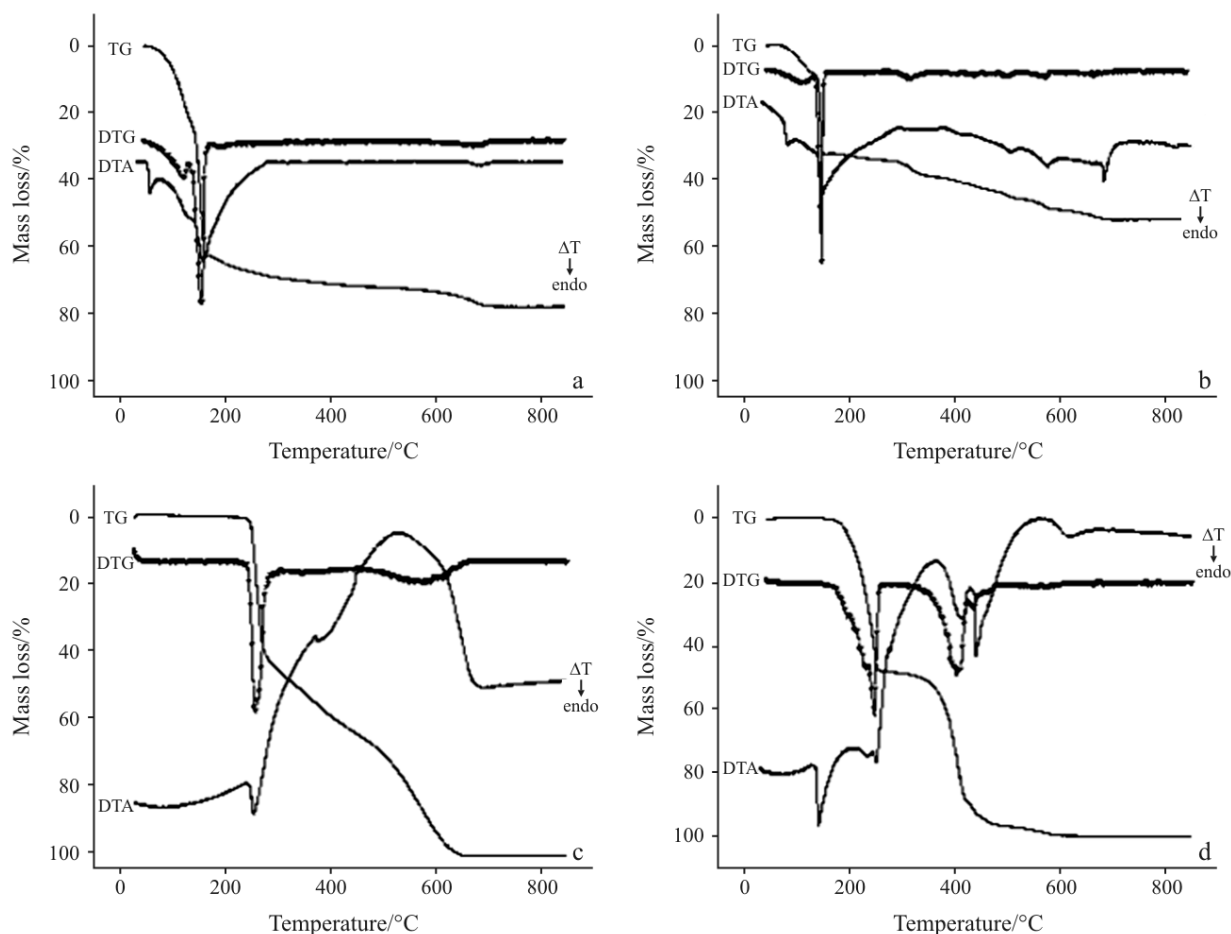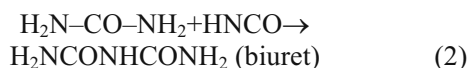
Fig. 1 The TG, DTG and DTA curves of the raw materials: a – Fe(NO$_3$)$_3$·9H$_2$O; b – Bi(NO$_3$)$_3$·9H$_2$O; c – glycine; d – urea

with $T_{\text{max DTG}}$=435.1 and 463.1°C and $T_{\text{max DTA}}$=439.3 and ~466°C (shoulder) and 481.9–610.0°C with $T_{\text{max DTG}}$=572.6°C and $T_{\text{max DTA}}$=608.0°C) characterized by mass losses of 8.31 and 3.81% are assigned to the decomposition of these condensation products.

$$H_2N–CO–NH_2+HNCO\rightarrow$$
$$H_2NCONHCONH_2 \text{ (biuret)} \quad (2)$$

$$H_2NCONHCONH_2+HNCO\rightarrow$$
$$H_2NCONHCONHCONH_2 \text{ (triuret)} \quad (3)$$

Thermal decomposition of the precursors

The investigated Fe(NO$_3$)$_3$·9H$_2$O–Bi(NO$_3$)$_3$·5H$_2$O–glycine and Fe(NO$_3$)$_3$·9H$_2$O–Bi(NO$_3$)$_3$·5H$_2$O–urea containing precursors, undergo in the temperature range 60–375°C/60–660°C a stepped decomposition (Figs 2a–c and 3a–c). The presence into the precursor of both reducing (glycine and urea) and oxidizing (NO$_3^-$) components, modifies dramatically their thermal behaviour comparative with the raw materials, both from the decomposition stoichiometries and temperature occurrence intervals points of view. Also, the thermal behaviour is dependent on the fuel nature but practically inde-

pendent with the fuel content. Several features which distinguish their thermal reactivity against the starting materials are important to be mentioned:

In the case of Fe(NO$_3$)$_3$·9H$_2$O–Bi(NO$_3$)$_3$·5H$_2$O–glycine system:

• The precursors are less stable (~60°C) than the free glycine (229°C), fact which indicates the occurrence of some self-propagating reactions since the start of the decomposition process [15, 16]. Also, the final decomposition temperatures which increases in the order 2.5 glycine (323.5°C)<3.5 glycine (374.7°C)<4.5 glycine (387.1°C) are several hundreds degrees lower comparative with the corresponding raw materials;

• The thermal decompositions are described by the existence of two main degradation stages. The first one, starts from ~60 up to ~200°C being characterized by a high mass loss (62–72%). This decomposition stage consists in an initial very weak endothermic effect (~140°C, shoulder) representing water evolving, followed by a fast and intensive exothermic process (~170°C), consisting in simultaneous evolving of NO$_3^-$ and glycine. Simultaneously, glycine is oxidized by nitrate anions [17].

The second decomposition stage, accompanied by a medium exothermic effect and mass losses of ~2–9%, represents the burn up of the remainder carbonaceous residue;

- The absence of phase transformations typical for the thermal behaviour of Bi_2O_3 (melting, $\alpha \rightarrow \delta$

Bi_2O_3), proves that all bismuth is included into mixed oxides.

In the case of $Fe(NO_3)_3 \cdot 9H_2O – Bi(NO_3)_3 \cdot 5H_2O –$ urea precursors

- No dramatic decrease of the precursors initial/final decomposition temperatures (in comparison with the raw materials' ones) is noticed;
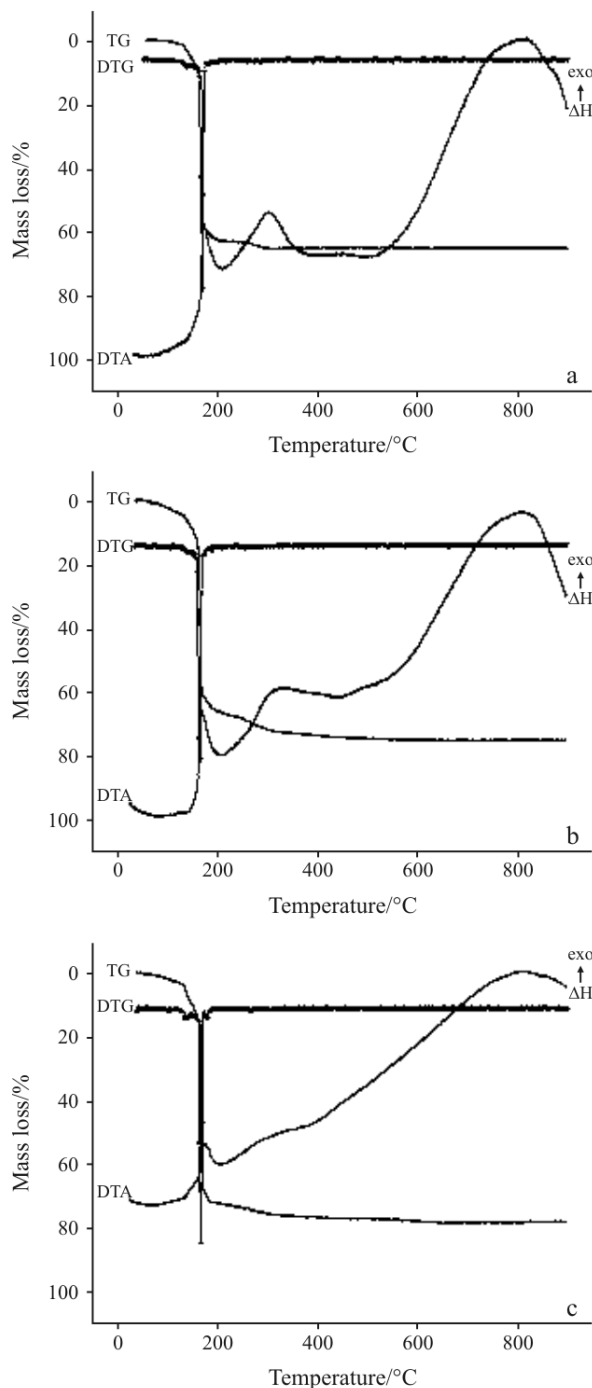

Fig. 2 Thermal behaviour of $Fe(NO_3)_3 \cdot 9H_2O – Bi(NO_3)_3 \cdot 5H_2O –$ glycine containing precursors:
a – $Fe(NO_3)_3 \cdot 9H_2O – Bi(NO_3)_3 \cdot 5H_2O – 2.5$ glycine;
b – $Fe(NO_3)_3 \cdot 9H_2O – Bi(NO_3)_3 \cdot 5H_2O – 3.5$ glycine;
c – $Fe(NO_3)_3 \cdot 9H_2O – Bi(NO_3)_3 \cdot 5H_2O – 4.5$ glycine

Fig. 3 Thermal behaviour of $Fe(NO_3)_3 \cdot 9H_2O – Bi(NO_3)_3 \cdot 5H_2O –$ urea containing precursors: a – 1:1:4; b – 1:1:6; c – 1:1:8

- Four main decomposition stages of the precursors are identified. The first one, (~60–~160°C) consisting in two overlapped mass loss processes ($T_{max\ DTG}$~85 and 115°C), and associated with three endothermic effects ($T_{max\ DTA}$~85, 115 and 150°C) is attributed to the evolving of water, part of urea and urea melting. The second (~160–~200°C) and the third (~200–~310°C) decomposition stages, characterized by exothermic effects are assigned to a simultaneous release of urea and decomposition of nitrate ions. A final oxidation of the carbonaceous residue occurs in the last decomposition step (~310–~660°C);

- In the case of the Fe(NO$_3$)$_3$·9H$_2$O–Bi(NO$_3$)$_3$·5H$_2$O–8 urea precursor thermal decomposition, a mass increase of 0.91% is registered in the temperature range 660–1000°C, process assigned to Fe^{2+}→Fe^{3+} oxidation (0.33 moles O$_2$). The presence of Fe^{2+} in the investigated system is determined by its higher content of the fuel (urea), which during the decomposition reactions reduces both the nitrate ions and the initial Fe^{3+};

- Similar with the thermal behaviour of Fe(NO$_3$)$_3$·9H$_2$O–Bi(NO$_3$)$_3$·5H$_2$O–glycine precursors, no phase transformations are evidenced.

Mixed oxide characterization

The room temperature X-ray diffraction patterns for the powders prepared using glycine as fuel and annealed for three hours at different temperatures show the evolution of both the interaction processes and the phase composition. For powders annealed at lower temperatures (500°C) only small amounts of BiFeO$_3$ were detected, beside some non-equilibrium compounds such as Bi$_2$O$_3$, Fe$_2$O$_3$, Bi$_2$Fe$_4$O$_9$, Bi$_{36}$Fe$_2$O$_{57}$, showing that in this temperature range, rather the kinetics and not the thermodynamic aspects influence the phase composition (Fig. 4). The increase of the annealing temperature leads to the increase of the intensity of the main diffraction peaks of BiFeO$_3$, which indicates that the solid-state reactions are in progress. However, even after annealing at 650°C these powders are not single phase, so that beside the BiFeO$_3$ major phase, amounts of secondary phases (Bi$_2$Fe$_4$O$_9$, Bi$_{36}$Fe$_2$O$_{57}$) were also identified (Fig. 4).

In the case of the oxides prepared using urea as fuel, a faster evolution toward a single phase composition with the temperature rise was pointed out by the X-ray diffraction patterns (Fig. 5). It is worthy to mention that in this case, the formation of the BiFeO$_3$ oxide phase is completed in the temperature range of 500–550°C. The further increase of the annealing temperature does not influence significantly the phase composition, so that the powders thermally treated at tem-
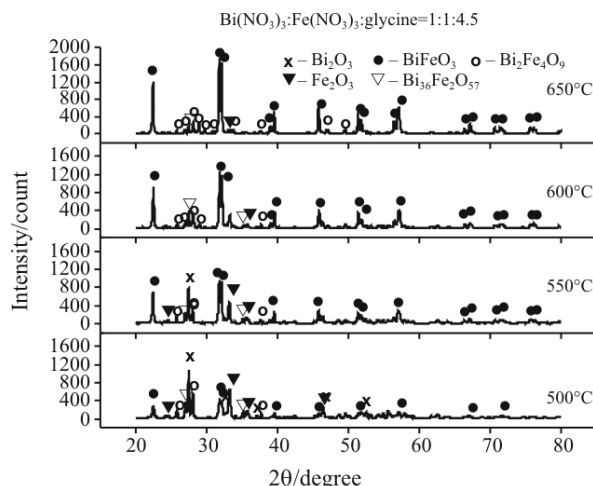

Fig. 4 Room temperature X-ray diffraction patterns of the oxides powders obtained from Bi(NO$_3$)$_3$–Fe(NO$_3$)$_3$–4.5 glycine system, annealed at for 3 h at various temperatures (BiFeO$_3$ – JCPDS no. 73-0548; Bi$_2$Fe$_4$O$_9$ – JCPDS no. 25-0090; Bi$_2$O$_3$ – JCPDS no. 71-0467; Fe$_2$O$_3$ – JCPDS no. 84-0308; Bi$_{36}$Fe$_2$O$_{57}$ – JCPDS no. 42-0181)
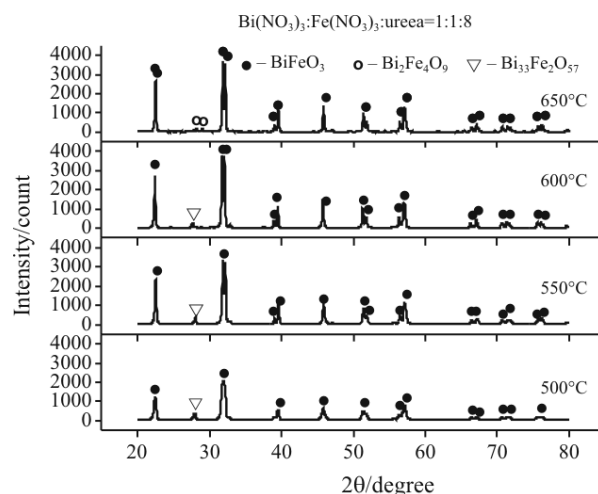

Fig. 5 Room temperature X-ray diffraction patterns of the oxides powders obtained from Bi(NO$_3$)$_3$–Fe(NO$_3$)$_3$–8 urea system, annealed for 3 h at various temperatures

peratures ranged between 550–650°C were almost single phase. It is interesting to note that for these compounds, the non-equilibrium Bi$_{36}$Fe$_2$O$_{57}$ forms at lower temperatures (500–550°C) and is consumed in the temperature range of 600–650°C when the Bi$_2$Fe$_4$O$_9$ compound starts to form. Therefore, after annealing at 650°C only traces of Bi$_2$Fe$_4$O$_9$ were detected.

Even if the particles are very small (at nanometric scale) so that the particle average size cannot be estimated by SEM, however this method provides useful information about the aggregation mode of these powders (Figs 6 and 7). For both oxidic powders a high tendency of agglomeration was noticed, but the morphology of the aggregates is quite different. Thus, while the powder
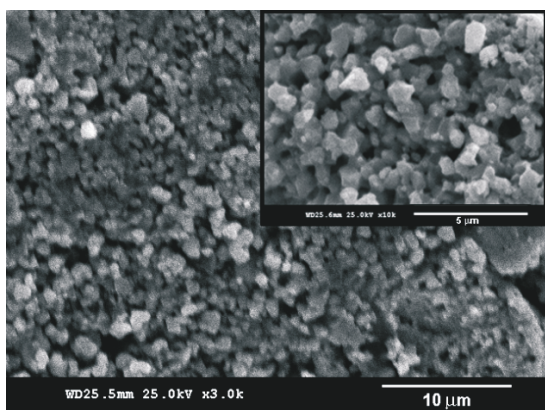
Fig. 6 SEM image of the oxide powder obtained from
Bi(NO$_3$)$_3$–Fe(NO$_3$)$_3$–8 urea system, annealed at
650°C/3 h

prepared using urea as fuel exhibits uniform (as shape
and size) and rather isolated agglomerates (inset of
Fig. 6), the particles aggregates of the powder prepared
using glycine as fuel show a non-homogenous morphol-
ogy and are strongly interconnected in a kind of
three-dimensional, porous skeleton similar to the struc-
ture of some ceramic foams (inset of Fig. 7). The last
type of morphology was observed for the BiFeO$_3$ pow-
der synthesized also by the combustion method, but us-
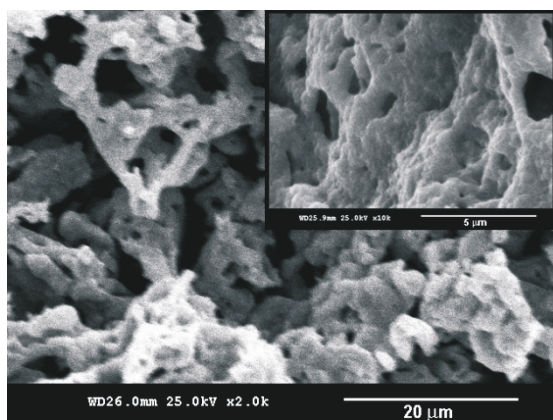ing α-alanine as fuel [18].

Fig. 7 SEM image of the oxide powder obtained from
Bi(NO$_3$)$_3$–Fe(NO$_3$)$_3$–4.5 glycine system, annealed at
650°C/3 h

Conclusions

Combustion method may represent a suitable route in
the synthesis of nanosized BiFeO$_3$ at temperatures
lower than 650°C. The fuel nature, glycine or urea
strongly influences the thermal behaviour of the pre-
cursors and some characteristics of the resulted ox-
ides (phase composition, morphologies). Starting
from glycine containing system, after annealing at

650°C, amounts of secondary phases (Bi$_2$Fe$_4$O$_9$,
Bi$_{36}$Fe$_2$O$_{57}$) were also identified beside the BiFeO$_3$
major phase. The particles of the obtained BiFeO$_3$
present a non-homogenous morphology being
strongly interconnected in a kind of three-dimen-
sional, porous skeleton. In the case of urea containing
system, after annealing at 650°C only traces of
Bi$_2$Fe$_4$O$_9$ were detected along with uniform, as shape
and size BiFeO$_3$ particles. The fuel content may influ-
ence the particle size and the reduction of Fe^{3+} to Fe^{2+}
of BFO. Thus, further transmission electron micros-
copy (TEM) and Mössbauer investigations are re-
quired in order to determine the particle average size
and the presence/absence of Fe^{2+} into BiFeO$_3$ pow-
ders prepared by the combustion method.

References

1 M. Mahesh Kumar, V. R. Palkar, K. Srinivas and
   S. V. Suryanarayana, Appl. Phys. Lett., 76 (2000) 2764.
2 G. Achenbach, W. J. James and R. Gerson, J. Am. Ceram.
   Soc., 8 (1967) 437.
3 I. Szafraniak, M. Połomska, B. Hilczer, A. Pietraszko and
   L. Kępiński, J. Eur. Ceram. Soc., 27 (2007) 4399.
4 S. Shetty, V. R. Palkar and R. Pinto, Pranama J. Phys.,
   58 (2002) 1027.
5 S. Ghosh, S. Dasgupta, A. Sen and H. Sekhar, J. Am.
   Ceram. Soc., 88 (2005) 1349.
6 X. Y. Zhang, J. Y. Dai and C. W. Lai, Prog. Solid State,
   33 (2005) 147.
7 C. Chen, J. Cheng, S. Yu, L. Che and Z. Meng, J. Cryst.
   Growth, 291 (2006) 135.
8 N. Das, R. Majumdar, A. Sen and H. S. Maiti, Mater.
   Lett., 61 (2007) 2100.
9 M. Malecki, R. Gajerski, S. Łabuś, B. Prochowska-Klisch
   and K. T. Wojciechowski, J. Therm. Anal. Cal.,
   60 (2000) 17.
10 M. Mrozek, Z. Rzączyńska and M. Sikorska-Iwan,
   J. Therm. Anal. Cal., 63 (2001) 839.
11 O. Carp, D. Gingasu, I. Mindru and L. Patron,
   Thermochim. Acta, 449 (2006) 55.
12 P. C. Srivastava, B. N. Singh, S. K. Ghosh and
   N. C. Ganguly, J. Thermal Anal., 31 (1986) 1153.
13 A. Kozak, K. Wieczorek-Ciurowa and K. Pielichowski,
   J. Thermal Anal., 45 (1995) 1245.
14 O. Carp, Rev. Roum. Chim., 46 (2001) 735.
15 C. Nenitescu, Organic Chemistry (in Roumanian) Ed.
   Didactica si Pedagogica, 1966, p. 832.
16 O. Carp, L. Patron, L. Diamandescu and A. Reller,
   Thermochim. Acta, 390 (2002) 169.
17 C. H. Yan, Z. G. Xu, F. X. Xheng, Z. M. Wang, L. D. Sun,
   C. S. Liao and J. T. Jia, Solid State Commun.,
   111 (1999) 287.
18 V. Fruth, D. Berger, C. Matei, A. Ianculescu, M. Popa,
   E. Ţenea and M. Zaharescu, J. Phys. IV 128 (2005) 7.